Research in Engineering Design (2026) 37:23
https://doi.org/10.1007/s00163-026-00485-1

ORIGINAL ARTICLE

Deriving Design Robustness Index: a model-based method for evaluating the robustness of product concepts

Jiahang Li[1] · Dennis Horber[2] · Fehmi Demir[1] · Philip Renner[1] · Patric Grauberger[1] · Stefan Goetz[2] · Sandro Wartzack[2] · Sven Matthiesen[1]

Received: 4 January 2025 / Revised: 3 April 2026 / Accepted: 11 April 2026

Abstract

Robustness against geometric deviations is a crucial success factor in product development. While early-stage Robust Design (RD) methods aim to improve robustness to reduce later costly iterations, they often fail to quantify the impact of concept-specific geometric deviations on the functional fulfillment of product concepts. This paper presents an Embodiment Function Relation and Tolerance (EFRT)-based method for quantitatively evaluating the robustness of product concepts against geometric deviations. Using the EFRT-based method, the Design Robustness Index is derived through a six-step process as a quantitative measure to evaluate and compare the robustness of different concepts. A case study of a coining machine demonstrates the practical application of the method. The indices generated by the method are initially validated through a comparison with empirical testing consisting of rapid prototyping and simulation with surrogate models. The results show a strong alignment between theoretical evaluation and empirical testing for the 16 different concepts. The proposed method can support design engineers in quantitatively evaluating how product concepts respond to geometric deviations in the early development stages, giving them a stronger foundation to make informed design decisions. It has the potential to reduce the risk of costly iterations caused by geometric deviations and ensure more reliable products.

Keywords Design methods · Product development · Robustness evaluation · Modeling method · Design knowledge

✉ Jiahang Li
jiahang.li@kit.edu

Dennis Horber
horber@mfk.fau.de

Fehmi Demir
fehmi.demir@student.kit.edu

Philip Renner
philip.renner@student.kit.edu

Patric Grauberger
patric.grauberger@kit.edu

Stefan Goetz
goetz@mfk.fau.de

Sandro Wartzack
wartzack@mfk.fau.de

Sven Matthiesen
sven.matthiesen@kit.edu

[1] IPEK-Institute of Product Engineering, Karlsruhe Institute of Technology (KIT), Kaiserstraße 10, 76131 Karlsruhe, Germany

[2] KTmfk-Engineering Design, Friedrich-Alexander-Universität Erlangen-Nürnberg (FAU), Martensstraße 9, 91058 Erlangen, Germany

1 Introduction

To remain competitive in today's dynamic markets, products must reliably fulfill their intended functions. However, various deviations, such as manufacturing variances, temperature fluctuations, or wear and tear, can prevent a product from functioning as expected (Geis et al. 2015). Product failures during their usage can endanger the companies producing them through recall costs or lawsuits. Product robustness, defined as insensitivity to various deviations (Taguchi et al. 2005), is therefore a critical success factor for a company. Mostly, issues of robustness are discovered late in the product development, e.g., in the testing phase. This results in significant costs and delays in the development project (Eifler and Howard 2018; Gremyr and Hasenkamp 2011). To minimize costly iterations due to robustness issues, they must be identified as early in the project as possible (Hasenkamp et al. 2009).

Robust Design (RD) comprises a variety of approaches aimed at enhancing product development by improving the insensitivity of functional fulfillment of a product.

Published online: 04 May 2026

While traditional RD methods primarily aim to optimize design parameters through experiments and simulations, prior research has shown that the principles and applications of RD are relevant across all stages of product development (Arvidsson and Gremyr 2008; Hasenkamp et al. 2009). Several researchers have emphasized that design decisions made during the conceptual and system design phases critically influence the robustness achievable in later stages (Andersson 1997; Brix et al. 2025). Recent reviews further highlight the growing attention devoted to RD in early design stages (Eifler and Schleich 2021), while also noting that existing methods still offer limited methodological guidance and support for these phases (Jugulum and Frey 2007; Gremyr and Hasenkamp 2011; Eifler and Howard 2018).

Despite this recognition, current early-stage RD approaches insufficiently address geometric deviations and their impact on product functionality. In particular, they lack quantitative evaluation to assess how concept-specific deviations influence functional fulfillment of a product, limiting design engineers' ability to evaluate the robustness of product concepts.

The contribution of this paper is the introduction of a novel robustness evaluation method, which is designed to systematically and quantitatively assess the robustness of product concepts against geometric deviations in early development stages. The proposed method provides design engineers with a stronger foundation for evaluating concept robustness and making informed design decisions. It has the potential to reduce the risk of costly design iterations caused by geometric deviations and ensure more robust and reliable products.

2 Related work and state of the art

In Sect. 2.1, the existing literature on robust design is reviewed, with an emphasis placed on current methodologies and key limitations. Based on these insights, the state of the art is summarized and the research question is formulated in Sect. 2.2.

2.1 Robust design in product development

RD can be applied throughout the product development process (Arvidsson and Gremyr 2008). As there is no uniform description of phases in product development, this paper focuses on the literature-based descriptions. Taguchi et al. (2005) categorize three main phases for RD: system design, parameter design, and tolerance design. Pahl et al. (2007) outline the product development process as consisting of task clarification, conceptual design, embodiment design, and detail design. Other researchers, e.g., Andreasen et al. (2015) or Brown (2008) also identify different stages, often related to specific development goals.

In this paper, the early stages of product development are defined as the period between ideation and parameterization (see Fig. 1). During these stages, design engineers must make a variety of critical design decisions, including defining the preliminary geometry of the product concept. These decisions are often guided by mental models formed during ideation. Although the preliminary geometry is roughly dimensioned by design engineers at this stage, the focus remains on defining the parameter space in which an optimal solution will later be explored through iterative refinement during the final parameterization phase. Consequently, these early design decisions have a significant impact on functional fulfillment and require careful attention from design engineers (Ullman 2010).

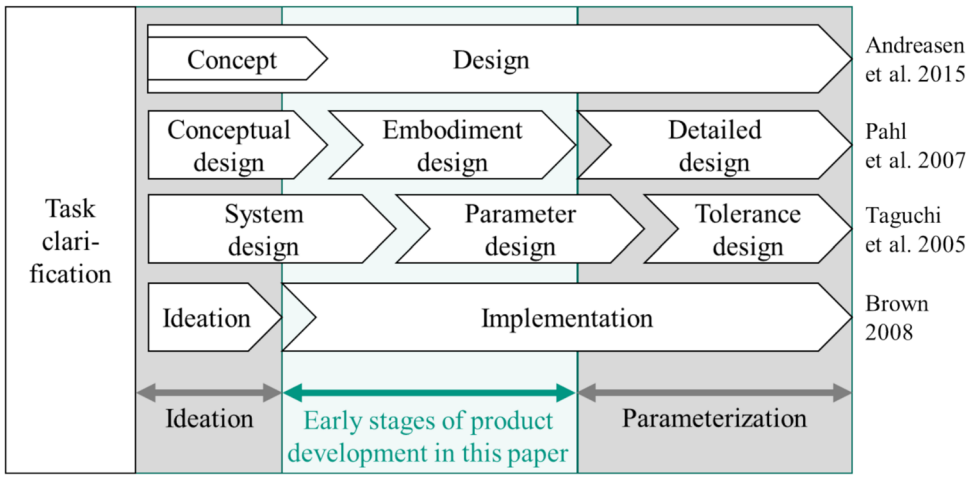

Fig. 1 Process of product development according to Andreasen et al. (2015), Pahl et al. (2007), Taguchi et al. (2005) and Brown (2008). The early stages of product development are defined as the period between ideation and parameterization for this paper

Some methods support the ideation phase in engineering design, such as the 6-3-5 method (Petersson and Lundberg 2018) or brainstorming (Hatcher et al. 2018). These techniques aid in generating ideas, but the created concept must then be refined into a product that can be realized. In mechanical product design, this involves defining the geometry of the concept, followed by detailed design with parameterization (Pahl et al. 2007). However, the phase between ideation and detailed design, where geometry needs to be defined but parameterization is not yet required, typically depends on the intuitive decisions of design engineers and often lacks methodical support (Goetz et al. 2020).

Traditional methods of RD primarily focus on parameterization at later stages of development, where a well-defined geometry is available (Gremyr and Hasenkamp 2011). In these phases, parameters can be optimized for robustness through experimentation and simulation (Phadke 1989; Taguchi et al. 2005). For example, the signal-to-noise ratio can be calculated based on experimental data to evaluate a product's robustness against various noise factors (Taguchi et al. 2005). However, early-stage design decisions have a critical impact on overall robustness, product performance, and cost (Andersson 1997; Ullman 2010). This goes along with the common understanding that early design decisions largely define the final characteristics and costs of a product. Early robustness considerations can help prevent costly concept changes and stringent tolerance requirements. A proper concept design should consider multiple different solutions, which should be selected with respect to product requirements and constraints. The aspect of robustness is one of these requirements and should therefore be considered at this stage, even though it cannot rely on final quantitative characteristics. Although early RD is essential for developing robust products, its implementation in practice remains challenging due to limited quantitative information (Eifler and Schleich 2021; Jugulum and Frey 2007).

Considering deviations in the early stages of product development is essential for RD, as deviations can impact a product's functional performance (Hasenkamp et al. 2009). Among various sources of variation, geometric deviations are particularly common and critically influence product quality and functionality. For this reason, they are the primary focus of this paper. Geometric deviations can be limited by specifying tolerance requirements to ensure the product quality (Morse et al. 2018). Typically, computer-aided workflows for detailed tolerance simulations are used to evaluate the defined product design (Qin et al. 2017). While tolerance management ensures product quality, it does not inherently improve robustness, as robustness is determined by the design itself. Attempting to compensate for non-robust designs by tightening tolerances is both challenging and costly (Ebro and Howard 2016).

Several methods have been developed to support the early consideration of deviations, including Variation Risk Management (Thornton 2004), Variation Mode and Effects Analysis (VMEA) (Johansson et al. 2006), and early error detection based on knowledge graphs (Faheem et al. 2023). These methods are useful for identifying deviations early in the design process but do not directly support design tasks. Mathias et al. (2011) further advanced this field with the introduction of the Robustness Ratio, an approach for assessing the robustness of a functional principle once its underlying physical relationships are understood. While these methods are valuable for identifying deviations and analyzing their impact, thus enabling targeted measures to mitigate these effects, they fall short in evaluating robustness against geometric deviations, as they minimally consider the embodiment of individual concepts. To support design engineers in their decision-making process in the early stages of product development, expert-based RD principles can be used (Andersson 1997; Ebro and Howard 2016; Eifler and Howard 2017; Li et al. 2023). For instance, considering these principles can prevent systems from being either overdetermined or underdetermined (Eifler and Howard 2017). However, proving the effectiveness of these principles is challenging, as they contradict each other, and the link between these principles and the functional performance of individual product concepts is not well understood (Horber et al. 2024). For example, reducing design parameters and incorporating tolerance adjustment elements represent two different principles, and a trade-off must be considered when applying them (Li et al. 2023). Göhler and Howard (2015) and Goetz et al. (2019) have attempted to combine these principles into an evaluation matrix to allow for the simultaneous consideration of various principles in robustness evaluation. However, these methods still cannot be used to analyze the impact of potential geometric deviations on the functional behavior of the product concept. Therefore, there is a need for a method that can support the analysis of the relations between geometric deviations and functional behavior in the early design stages.

There are several approaches that support the analysis of the relations between a product's embodiment and its functions in the early stages of product development. Methods such as the Design Structure Matrix (DSM) (Eppinger et al. 1994), Axiomatic Design (Suh 1998) and Characteristic Property Modelling (CPM) (Weber 2014) investigate dependencies within the system architecture to assign different functions to components. By reducing the coupling of components for the same functions, the robustness of the system can be improved. The Function-Behaviour-Structure (FBS) framework proposed by Gero and Kannengiesser (2014) extends this mapping to include the functional behavior of a system. These approaches are well-suited for application during the system design phase, but they are

challenging to apply to early RD of the product geometry, as the often sketch-based graphical representations of a product concept are difficult to integrate into a matrix. Here, a graph-based approach has been proposed (Goetz et al. 2018). This approach breaks down the product concept into geometric elements and models the geometric relations in the product's structure. Based on the geometric relations in the derived graph, robustness of a product concept can be evaluated quantitatively with the approach introduced by Goetz et al. (2019). However, this evaluation also relies on a combination with RD principles and does not provide insights into functional behavior.

In early design stages, exploring the design space is crucial. Methods like enhanced function–means (EF-M) modeling systematically generate and analyze alternatives by enriching function modeling (Müller et al. 2019), while solution space engineering focuses on systematically exploring tolerances and uncertainties in design parameters to improve performance reliability (Zimmermann and Hoessle 2013). Margin-based approaches, introduced by Thunnissen and Tsuyuki (2004) and advanced in the Margin Value Method (MVM) (Brahma et al. 2022; Brahma and Wynn 2020), enable rigorous evaluation of design margins for robustness and flexibility under uncertainty. Building on MVM, Al Handawi et al. (2024) proposed a framework integrating EF-M with margin-based metrics to generate, evaluate, and rank large sets of feasible concepts by quantitatively balancing flexibility and performance trade-offs amid uncertainty. While these methods support systematic early design exploration, design engineers often face practical challenges in using the results from these methods to make informed decisions, particularly when estimating the impacts of geometric deviations on functional behavior during real-world design tasks.

To gain deeper insights into the functional behavior of a product concept, it is essential to distinguish cases based on whether geometric deviations introduce additional degrees of freedom (see Fig. 2). If the system, following the design guideline of Eifler and Howard (2017), is neither overdetermined nor underdetermined, and no additional degrees of freedom arise from the geometric deviations, the functional behavior can be directly inferred from the geometric relationships (see Fig. 2 on the left). However, if geometric deviations do introduce additional degrees of freedom, the functional behavior becomes dependent on these deviations (see Fig. 2 on the right). In such cases, traditional statistical variation analysis, relying solely on geometric relations, may yield overly broad parameter ranges due to the undefined behavior. In practice, the system behavior depends on the load path and typically exhibits less variability, significantly affecting the actual robustness of the product concept.

Functional behavior can be analyzed using the Contact and Channel Approach (C&C^2-A) (Matthiesen et al. 2019), although geometric deviations are not yet considered in this approach. The EFRT model combines the advantages of both the graph-based approach and the C&C2-A, enabling the analysis of the relations between geometric deviations and functional behavior (Horber et al. 2022; Li et al. 2024b). Further research already demonstrates the practical applicability of this model in industrial contexts (Kleinhans et al. 2024; Li et al. 2024d). The EFRT model currently lacks a quantitative method to evaluate robustness, making it difficult to directly compare the quality of multiple concepts. As a result, while the EFRT model shows significant potential for robustness evaluation, the development of a comprehensive quantitative method for comparing multiple concepts remains an open area of research.

2.2 Summary of the state of the art and research question

Many models and methods support RD, and some of them are specifically developed to be applicable in early RD.

To evaluate the robustness of a product concept during these stages, it is essential to thoroughly analyze and assess the relations between functional fulfillment and geometric deviations within a system. Functional fulfillment, a key aspect of robustness evaluation in this paper, is inherently linked to both the product's structure and its expected behavior (Gero and Kannengiesser 2014). While Goetz et al. (2019) address robustness from the perspective of geometric structures by evaluating the impact of geometric relations on product robustness, existing methods do not sufficiently assess robustness from the perspective of functional behavior. As a complement, the method proposed by Matthiesen et al. (2019) can be applied to assess system

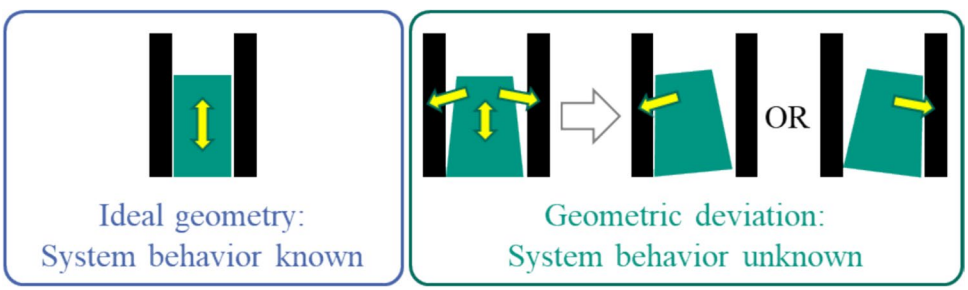

Fig. 2 Case distinction: geometric deviations may result in additional degrees of freedom and unknown system behavior

behavior, provided that specific geometric deviations are identified. The research gap lies in the lack of methods that quantitatively assess the robustness of product concepts by simultaneously considering both geometric structures and the functional behavior of the product concept. The EFRT model introduced by Horber et al. (Horber et al. 2022), which combines the advantages of the approaches of Goetz et al. (2019) and Matthiesen et al. (2019), has the potential to bridge this gap.

The problem is that, with existing methods, it is difficult for design engineers to quantitatively evaluate the robustness of product concepts against geometric deviations, limiting their ability to make reliable design decisions. Therefore, we have derived our research question:

Research question: *How can the robustness of product concepts against geometric deviations in the early stages of product development be quantitatively evaluated?*

To address the research question, a method for quantitative robustness evaluation in early RD is developed. In accordance with the Design Research Methodology framework by Blessing and Chakrabarti (2009), an initial validation of the proposed method is conducted in this contribution. This paper is structured as follows: In Sect. 3, the EFRT-based method for robustness evaluation is presented. This is followed by a validation study using a case study in Sect. 4. In the case study, the EFRT-based method for robustness evaluation is first applied to a coining machine to evaluate the robustness of various design concepts. The evaluated robustness is subsequently validated through testing. The results of the robustness evaluation and the testing are then compared. The insights and limitations are then discussed in Sect. 5. Conclusions are drawn in Sect. 6.

3 EFRT-based method for robustness evaluation—deriving the Design Robustness Index

This section introduces the EFRT-based method for robustness evaluation, which aims to address the research question. In Sect. 3.1, the EFRT model is presented as the foundational basis for the proposed approach. Section 3.2 then introduces the method proposed in this paper, outlining the objectives and expected outcomes of each step within the method.

3.1 The embodiment function relation and tolerance model

As the EFRT model shows a high potential for application in early RD, it is introduced in more detail in this section. The EFRT model aims to represent the relation between geometric deviations and functional fulfillment within a product concept, as illustrated in Fig. 3. The EFRT model is composed of two primary components: the EFRT graph and the EFRT sketch, which together model the product concept and associated geometric deviations. To evaluate functional fulfillment, the model employs the concept of Key Characteristic (KC) as defined by Thornton (2004), which represents a quantifiable specification whose deviation significantly impacts functional fulfillment. The model integrates five key model elements: Key Characteristic (KC), Geometry Element (GE), Working Surface Pair (WSP), Contact and Support Structure (CSS), and Connector (C), as proposed by Li et al. (2024b). By modeling both geometric deviations and the resulting changes in KCs, the EFRT model provides a comprehensive qualitative evaluation of product concept robustness.

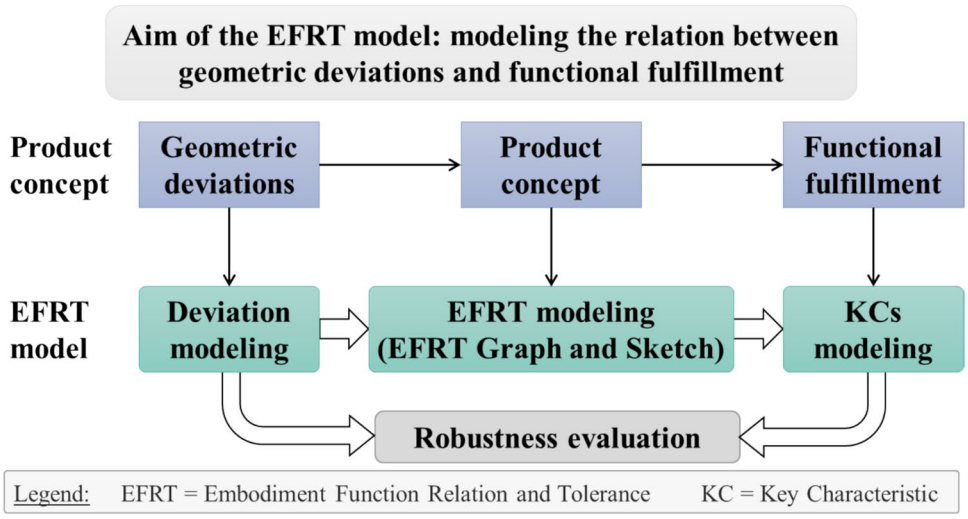

Fig. 3 The EFRT model aims to represent the relation between geometric deviations and functional fulfillment within a product concept

For a better illustration of the EFRT model, a hand-operated coining machine is used as an example, with its working principle depicted in Fig. 4a on the left. In this system, manual operation generates force by pressing the bars (3) and (4), causing the piston (5) to move downward while being guided by a cylindrical guide (6). During this downstroke, the coin, positioned on the bed (1), is minted by the piston. After the minting process, the system facilitates the release of the minted coin from the piston.

Figure 4a demonstrates the procedure to create the EFRT models, including the EFRT graph and EFRT sketch, for the example coining machine system, as explained below.

The EFRT graph models the system structure by decomposing the product into GEs and the geometric relations connecting them. The simplified procedure to create an EFRT graph is shown in Fig. 4a) (system structure modeling) and consists of the following steps. First, the assembly is divided into function-relevant parts, each assigned an identifier, for example the piston (5). Next, the relations between these parts are defined, such as a cylindrical joint between the bar (4) and the piston (5), or a prismatic joint between the piston (5) and the guide (6). The parts are then further decomposed into GEs, i.e., interacting surfaces. For instance, the piston (5) contains the hole (5a), skirt (5b), and crown (5c) as GEs. After that, the EFRT graph of the assembly is created by representing each GE as a node and connecting nodes with edges according to the identified geometric relations. These relations are stored as labels on the edges; for instance, the perpendicularity of the crown surface to the skirt surface is attached to the edge between (5c) and (5b). A more detailed description of the procedure for constructing EFRT graphs is provided in Li et al. (2024b). At the end of the coining state, the KC coin angle is defined by the angle between the piston crown (5c) and bed support surface (1a). As observed in the EFRT graph, this KC can be influenced by two distinct loops, from each of which a tolerance chain could be derived during detailed design phase. Importantly, KCs in this work represent functional behavior evaluated at the system level, not classical manufacturing tolerance chains. When multiple loops contribute to one KC, these represent alternative structural paths affecting the same functional behavior, rather than simultaneously enforced tolerance chains. While such

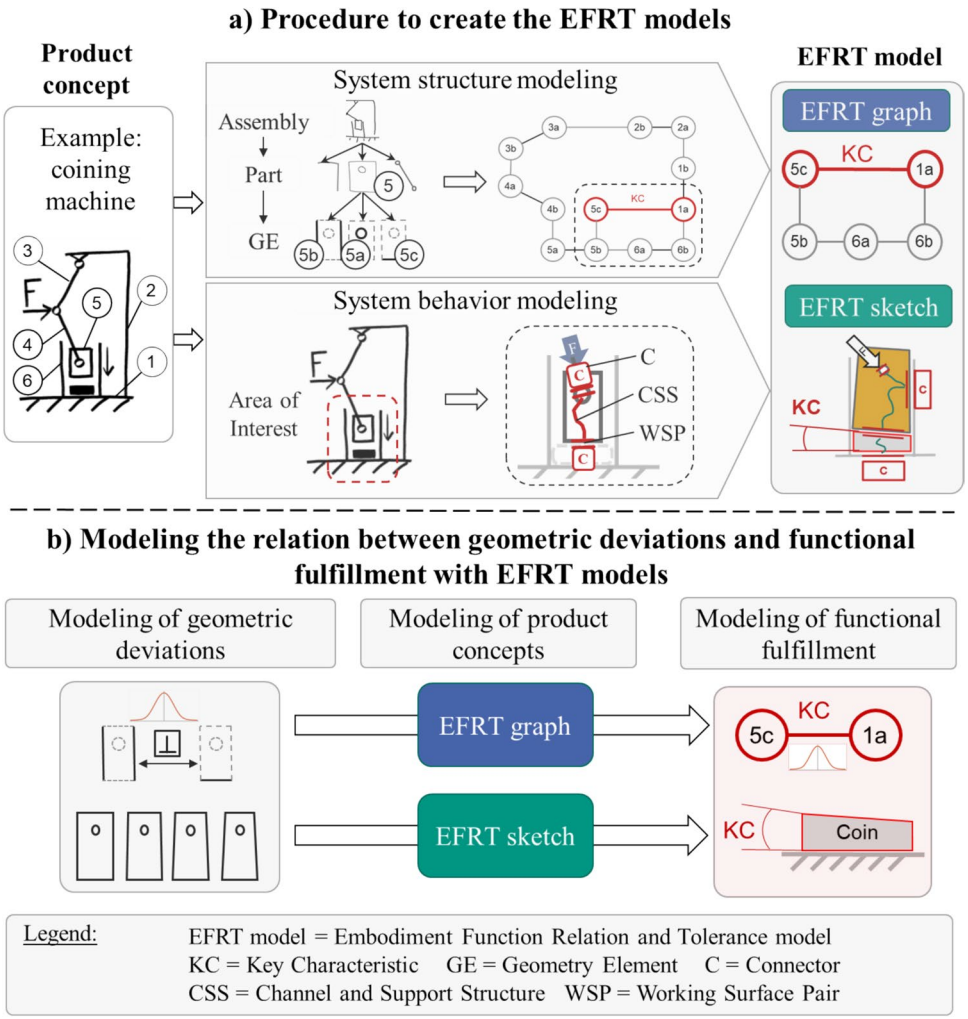

Fig. 4 Overview of building and applying the EFRT model illustrated with the example of a coining machine. The figure depicts a) the procedure to create the EFRT models based on system structure and behavior modeling and b) the modeling of the relation between geometric deviations and functional fulfillment. Functional fulfillment is represented using key characteristics (KCs). Certain elements of the figure are adapted from Li et al. (2024b)

configurations should be avoided for optimal robustness and tolerance traceability, they reflect realistic scenarios (e.g., car body structures, scissor lift mechanisms) (Goetz et al. 2018). To minimize the influence of individual GEs on the KC, the shortest functional loop surrounding the KC can be extracted for focused analysis, as proposed by Goetz et al. (2018).

The EFRT sketch models the system behavior under geometric deviations. To create an EFRT sketch, the designer first defines a "area of interest" within the product concept (see Fig. 4a, system behavior modeling) to limit modeling scope. This area is selected based on its critical role in function fulfillment. For example, the coining area including the piston (5), the guide (6) and the bed (1) is designated as the area of interest, as it directly affects coining quality and functional fulfillment. Once this area is defined and sketched, key C&C2-A elements (WSP, CSS, Connectors) are identified and incorporated into the EFRT sketch. For example, the minting force transmission is modeled as follows (Fig. 4a, system behavior modeling): starting with the WSP between lower bar and piston hole, the load path continues through the CSS in piston body, and ends at the output WSP (piston-coin contact), with Connectors representing boundary conditions (input force from the lower bar and support from bed. WSPs can be added or removed across different system states, enabling state-specific modeling of system behavior. To complete the EFRT sketch, critical geometric deviations are visualized at the relevant locations where they affect WSPs and CSSs. These deviations may alter contact conditions or load paths, with the resulting KC deviation indicated in the EFRT sketch (Fig. 4a, EFRT sketch). This visualization supports the detailed exploration of KC and its reliance on geometric characteristics.

Figure 4b illustrates how the created EFRT models (graph and sketch) are used to analyze the relations between geometric deviations and functional fulfillment. Geometric deviations are integrated into the EFRT graph and visualized within the EFRT sketch, as shown in Fig. 4b on the left. The impact of these deviations on KCs can be then modeled using both the EFRT graph and sketch. In an EFRT model, a KC can be assigned into the EFRT graph between GEs, or it can be drawn directly in the EFRT sketch (see Fig. 4b on the right). For the coining machine example, a KC is defined as the angle between the upper and lower surfaces of the coin, which is expected to be 0° for ideal functionality. Using the EFRT model, potential KC deviations can be modeled early in the design process.

For a more detailed description of the modeling process, the stage-gate process proposed by Li et al. (2024b) supports the step-by-step building and application of the EFRT model for robustness evaluation. This modeling process has already been evaluated as well applicable through a subject study (Li et al. 2024c).

3.2 The EFRT-based method for robustness evaluation

The EFRT-based method for robustness evaluation is tailored for early mechanical design stages, bridging ideation and detailed design, where geometry must be defined but detailed parameterization is not yet required. It focuses on robust analysis of design characteristics rather than conceptual exploration. The method consists of six steps, as shown in Fig. 5. The purpose of this structured robustness evaluation is to assess various design concepts in terms of their robustness against a specified geometric deviation. At the end of the method, a Design Robustness Index (DRI) is obtained, which enables a comparative evaluation of the robustness across different concepts. For improved clarity and understanding, its detailed application is demonstrated later in Sect. 3 through a case study.

Step 1: Define key characteristic (KC)

The aim of this step is to define a parameter that represents the quality of functional fulfillment, enabling the evaluation of how well the function is fulfilled. In this method, KC (see Sect. 2.1) is used as the evaluation metric for functional fulfillment. The KC lies within the so-called area of interest, which refers to the location critical to functional fulfillment and requires particular attention in the analysis. This area is delimited so that only the elements that primarily

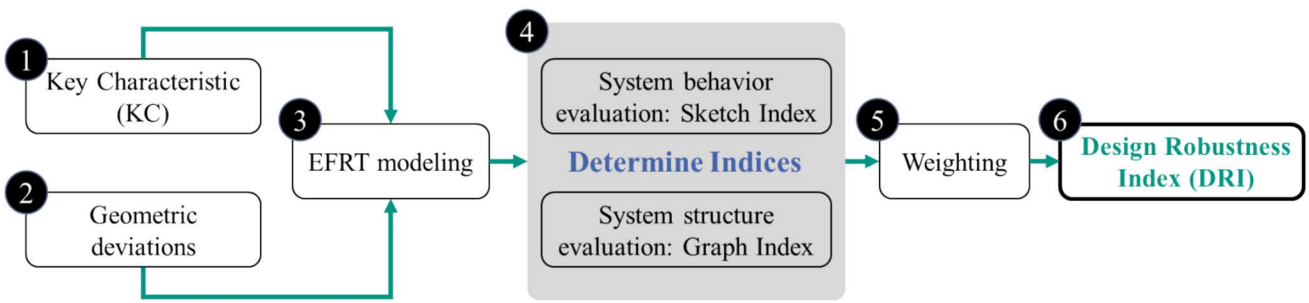

Fig. 5 The EFRT-based method for robustness evaluation has six steps to derive the Design Robustness Index

influence the functional performance are considered. For functional fulfillment, the KC has an ideal value that allows the function to be realized optimally. This ideal KC value is achieved with an ideal geometry. In reality, there is always a deviation from the ideal KC value, as the real KC value is influenced and determined by other deviations in the product geometry as well as the relevant system states. Deviation in the KC can lead to reductions in the functionality of the product, making it crucial to define the KC in this step. The output of this step is a defined KC or multiple KCs, whose deviations will be evaluated in later steps.

Step 2: Identify critical geometric deviations

The aim of this step is to identify critical deviations in the product concept, as these deviations can lead to impairments in functional fulfillment. Real components deviate from the ideal design due to factors such as manufacturing tolerances, assembly deviations, and other variations, which can cause the KC value to deviate from the ideal value. To answer the question of which concept is more robust under a given deviation, critical geometric deviations must be identified, such as form deviations or clearances. While geometric deviations generally fall within standard tolerances, certain critical deviations, caused by manufacturing or wear, may exceed these tolerances and typically have a greater impact on the KC. To identify the critical deviations, experience from previous product generations (Albers and Rapp 2022) should be considered. Specifically, design engineers need to identify potential deviations based on their knowledge of previous projects or reference products. Tools such as VMEA (Johansson et al. 2006) can assist in this assessment. The output of this step is the identification of critical geometric deviations, which will be further analyzed in the next step to assess their influence on the KC.

Step 3: Perform EFRT modeling

The aim of this step is to build the EFRT models (EFRT graph and sketch) for the product concepts, as these models serve as the foundation for robustness evaluation. This step is divided into two parts: evaluating the system structure through the EFRT graph and assessing the system behavior in the critical area through the EFRT sketch. An introduction to the EFRT sketch and graph can be found in Sect. 3.1. A more detailed description of how to build the EFRT model from different design situations is provided using the modeling method developed by Li et al. (2024b). As mentioned in Sect. 3.1, KC is integrated into the EFRT graph to identify the functionally relevant GEs (see Fig. 4a, EFRT graph). To determine the system behavior, state modeling is performed based on the EFRT sketch for the area of interest. Deviations in boundary conditions, inputs, and the system itself are considered to model and visualize the deviation of KC in the EFRT sketch (see Fig. 4a EFRT sketch). This modeling process helps to understand how the system will behave under the given conditions and deviations. The output of this step is the EFRT graph and sketches, which model the geometric deviations and KCs.

It is important to understand when state modeling is critical. In this paper, we assume that deviations within general tolerance limits do not introduce substantial additional degrees of freedom. In this case, the EFRT graph is sufficient for the evaluation. However, if some specific deviations introduce additional degrees of freedom, system behavior becomes influenced by these deviations. Therefore, state modeling is required to analyze the system behavior. In this case, the EFRT sketch is essential for examining system behavior under each specific deviation.

Step 4: Determine indices

The aim of this step is to determine the indices from the EFRT graph and sketch, enabling the quantification of the evaluation through these models. For both evaluating factors (system structure and system behavior), a separate performance indicator is determined. The output of this step includes the Graph Index (GI) and the Sketch Index (SI), which will be used together in the next step for robustness evaluation. The indices are intended as comparative, semi-quantitative indicators for early design stages rather than absolute measures of robustness.

The Graph Index evaluates whether the system structure of the product concept is well-structured or poorly structured. It is calculated by the number of GEs, i.e., the length of the functional chain (see Sect. 3.1), using the created EFRT graph. A longer functional chain, which contains more GEs, means more contributors to the KC, and therefore a higher risk of deviation in the KC. The concept with the longest chain (the highest number of GE) receives a value of 1 as its Graph Index. The remaining concepts receive Graph Index values within the range of 0–1, depending on the number of GE relative to the number of GE of the concept with the longest chain. This can be expressed as:

$$\textit{Graph Index}\,(GI) = \frac{\textit{Number of GE in current graph}}{\textit{Number of GE in graph with longest tolerance chain}} \quad (1)$$

The Graph Index implies a tendency toward reduced robustness with more contributors (longer chains), as each additional GE increases the probability of larger robustness losses through deviation propagation. However, this is a risk-oriented heuristic for early design phases where detailed tolerances and uncertainty data are unavailable, rather than a fixed rule applicable once such information becomes available.

The Sketch Index evaluates the functional behavior of the system under the identified critical deviations in relevant system states. It is calculated by evaluating the deviation in the KC across the concepts. This deviation can be influenced by variations in boundary conditions, the system, and input.

Through state modeling in the EFRT sketch from Step 3 and incorporating the critical deviations identified in Step 2, the deviation in KC (defined in Step 1) of the concepts from its ideal value has to be estimated using various physical laws. The concept with the greatest deviation receives a value of 1 as its Sketch Index. The remaining concepts are assigned Sketch Index values within the range of 0–1, based on their respective deviations from the ideal KC value. The Sketch Index for an individual deviation can be expressed as:

$$Sketch\ Index\ (SI) = \frac{Deviation\ of\ KC\ in\ current\ sketch}{Maximum\ deviation\ of\ KC\ across\ all\ sketches} \quad (2)$$

Due to limited availability of detailed tolerance, uncertainty, and statistical information in early design phases, the Sketch Index is not intended as an absolute measure of robustness. Instead, it enables a structured comparison of alternative concepts with respect to their sensitivity to critical deviations under varying boundary conditions, system states, and inputs.

For multiple individual deviations, the SI must be calculated separately for each deviation, while the Graph Index is calculated only once for the entire system structure.

Step 5: Define weighting factors

The aim of this step is to assign appropriate weighting factors to the indices derived in the previous step, enabling a unified evaluation using these indices. Each index (Graph Index and Sketch Index) is assigned a weighting factor, based on its importance in the overall system performance. The weighting factor is determined by evaluating how significant the identified deviation is compared to others, considering its impact on the KC. This involves considering the experience and know-how within the company regarding the manufacturing and assembly of components. Defining the weighting factors requires expertise and must be done context-specific to ensure that they accurately reflect the most critical aspects of the deviations for the specific application.

For simplicity and practical application in determining weighting factors, this paper adopts a four-point Likert scale, following Robbins and Heiberger (2011). The scale is defined as follows: Graph Index addresses general deviations and tolerances within the product concept. Tolerance class, defined as the allowable geometric deviations for a product's components, is a critical factor that affects both cost and functional fulfillment. These classes are determined by design engineers in accordance with company-specific requirements and practices. In this paper, the tolerance classes specified in ISO 2768-1 are used to determine the weighting factor of the Graph Index. On a scale of 1 to 4, this corresponds to fine, medium, coarse, and very coarse according to ISO 2768-1. A very coarse tolerance class requires compensation through a robust system structure design. Sketch Index focuses on specific deviations that impact functional behavior which were identified in Step 2. These deviations often exceed general tolerances or specific tolerance specifications due to factors like manufacturing variations or wear and tear, demanding additional attention. Thus, the probabilities of occurrence that these specific deviations exceed the tolerance specifications, identified in Step 2, are weighted. On a scale of 1 to 4, this corresponds to very small, small, large, and very large probability. Based on company-specific experience, design engineers can also individually adjust these weighting factors as needed. While the weighting factors are necessarily subjective, their structured definition enhances transparency, consistency, and repeatability within a given organizational context.

The output of this step is the assignment of a weighting factor to each index, which will be used in the next step for the final robustness evaluation.

Step 6: Calculate Design Robustness Index (DRI)

The aim of this step is to combine the indices from Step 4 using the weighting factors from Step 5, allowing for an evaluation of the robustness of a product concept considering both system structure and system behavior. The Design Robustness Index (DRI) is calculated by summing the products of each weighting factor with its corresponding Graph Index and Sketch Index. Suppose the weighting factor for the Graph Index is denoted as a, and the weighting factors for each individual deviation's Sketch Index are denoted as b_i. Then, the DRI can be calculated as:

$$Design\ Robustness\ Index\ (DRI) = a \cdot GI + \sum_{i=1}^{n} b_i SI_i \quad (3)$$

It is important to note that a higher DRI value indicates lower robustness. Therefore, as the DRI increases, the robustness of the product concept decreases. After completing Step 6, the DRI is derived and compared across all evaluated product concepts to enable informed design decisions. Through systematic analysis and comparison of product concepts using EFRT graphs and sketches, design engineers gain deeper insights into the relative robustness of different concepts. This knowledge supports subsequent synthesis steps. For instance, design engineers may select the concepts with the lowest DRI for further consideration, or alternatively, identify how concepts with higher DRIs can be optimized through design modifications to yield more robust solutions. In such cases, the newly generated concepts undergo comparison with the existing ones, and new DRIs are derived to guide the final design decision.

4 Case study for an initial validation of the EFRT-based robustness evaluation

This section addresses the initial validation of the indices derived through the EFRT-based method within a case study involving a coining machine. The robustness evaluation is first conducted, and the resulting Graph Indices and Sketch Indices are validated through testing.

The process of the validation study is shown in Fig. 6. First, different concepts of the coining machine, in which the robustness needs to be evaluated, are presented (see Fig. 6, at the top). During the design of the coining machine, various design decisions must be made. In this paper, four typical design decisions should be made concerning four different design characteristics (see Fig. 6 Step 1 on the right): the connecting rod length (long or short), the borehole position in the piston (top or bottom), the length of the guide elements (long or short), and the connection of the guide (to the bed or frame). With these four design decisions and two options for each, a total of 16 concepts result, as shown in Fig. 6. According to the p-diagram framework described by Jugulum and Frey (2007), the design characteristics listed are designated as control factors decided by designers, while geometric deviations act as noise factors. In this system, the input signal corresponds to the crank rotation, and the output response is the coining angle, which represents the coining quality and requires evaluation. The robustness of these 16 concepts needs to be evaluated.

In Step 2 (see Fig. 6, middle left), the robustness of the product concepts is evaluated by the authors using the EFRT-based method, resulting in different DRIs. It is important to assess how the subjective robustness evaluation by the authors aligns with the objective measurement of

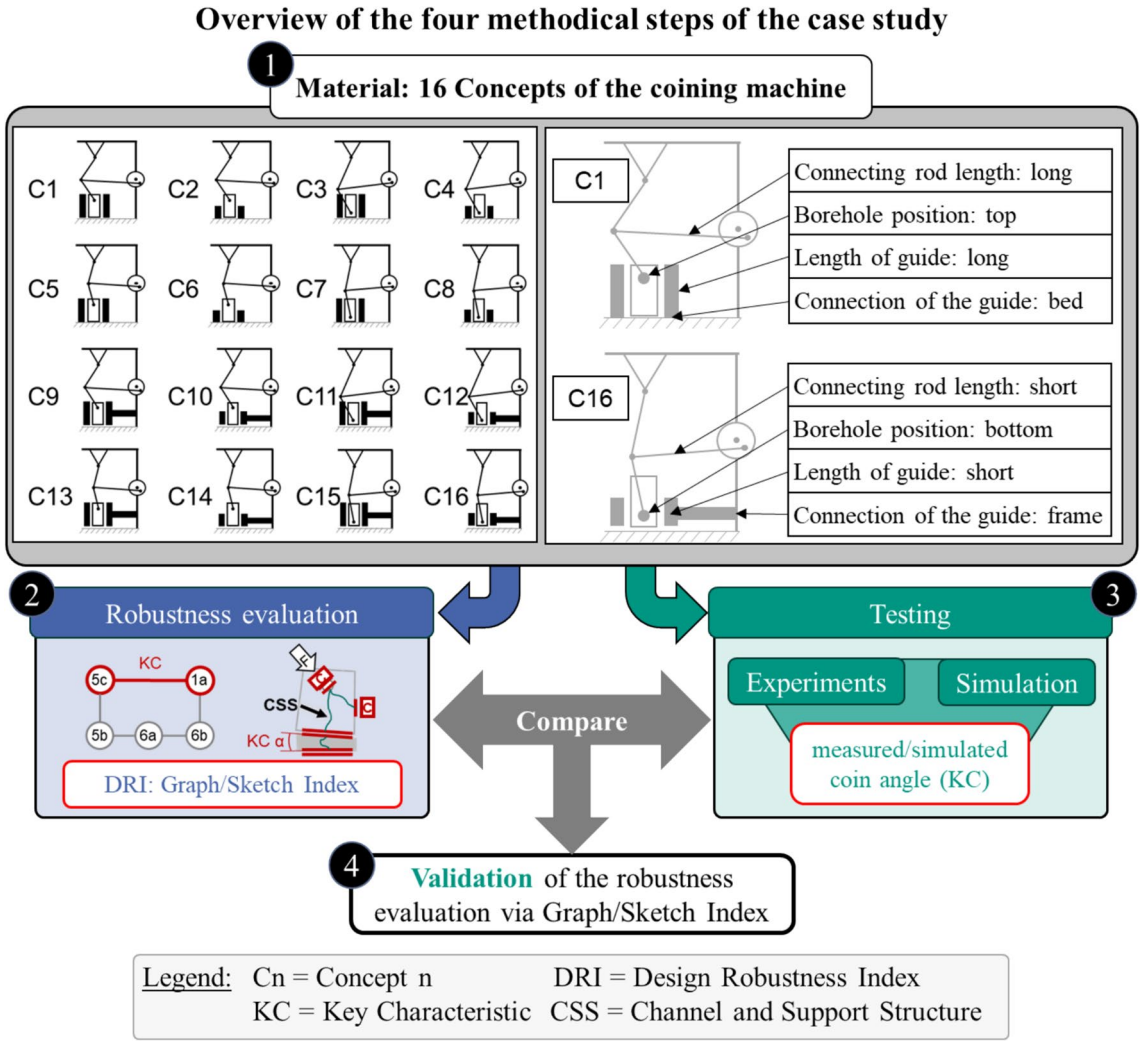

Fig. 6 Case study for an initial validation of the robustness evaluation: 16 concepts of the coining machine are evaluated with the EFRT-based method, and the evaluation results are compared with the testing results

robustness for the coining machine. As described in Sect. 3, KC is the key parameter for robustness evaluation. To measure KC early in the development phase, preliminary testing is conducted using surrogate models. This testing is carried out either through experiments or simulations in Step 3 (see Fig. 6, middle right). The selection of the testing methods is then explained. In the final Step 4 (see Fig. 6, at the bottom), the Graph Indices and Sketch Indices are compared with the measured or simulated KCs to validate the robustness evaluation.

4.1 Robustness evaluation for the coining machine

The robustness of the 16 coining machine concepts was evaluated systematically using the EFRT-based method for robustness evaluation, as described below. The exemplary procedure for Concept 1 is shown in Fig. 7.

In Step 1, a KC for the coining machine was defined. For this case study, the KC is the angle between the coin's upper and lower surfaces, as it directly reflects the coin's quality (see Fig. 7). The ideal value for the KC is 0°. Deviations from this value indicate a reduction in functional fulfillment, with larger angles correlating to poorer functional outcomes. The KC value is influenced by the geometric deviations and system states defined in the subsequent steps. Consequently, the KC values vary across different coining machine concepts due to differences in their tolerance chains, which are represented by the EFRT graphs, and system states, which are visualized in the EFRT sketches, both resulting from distinct designs.

In Step 2, the relevant geometric deviations to be analyzed were identified. In the ideal state, all concepts of the coining machine inherently include minor deviations that fall within the general tolerance limits specified by ISO 2068-1, reflecting standard manufacturing tolerances. However, due to limitations in manufacturing processes, some deviations frequently exceed these tolerances. To reduce rejection rates caused by such deviations, the coining machine should be designed to be robust against them. Two specific types of deviations were selected for this study: piston shape deviation and clearance deviation (see Fig. 7), as these commonly result from manufacturing inaccuracies or wear over time. For piston shape deviation, the ideal state is that the side and bottom edges of the piston are perpendicular. To evaluate robustness, an angular deviation of 5° from this rectangle was introduced. For clearance deviation, the ideal state involves a fit of H7/m6 between the piston and guide. To evaluate robustness against this deviation, an increased clearance of 2 mm was analyzed. Based on previous experience, other geometric deviations within the system are considered less critical to exceed standard manufacturing tolerances. The deviation magnitudes used in this case study are intentionally amplified to clearly demonstrate the proposed method's capability to evaluate the influence of geometric deviations at the concept stage. These values should not be interpreted as nominal manufacturing tolerances, but rather as representative of potential operational or wear-induced deviations. In early design phases, exact tolerance values are typically unknown and are defined only in later stages; therefore, the objective here is to analyze relative sensitivities and robustness trends rather than absolute numerical

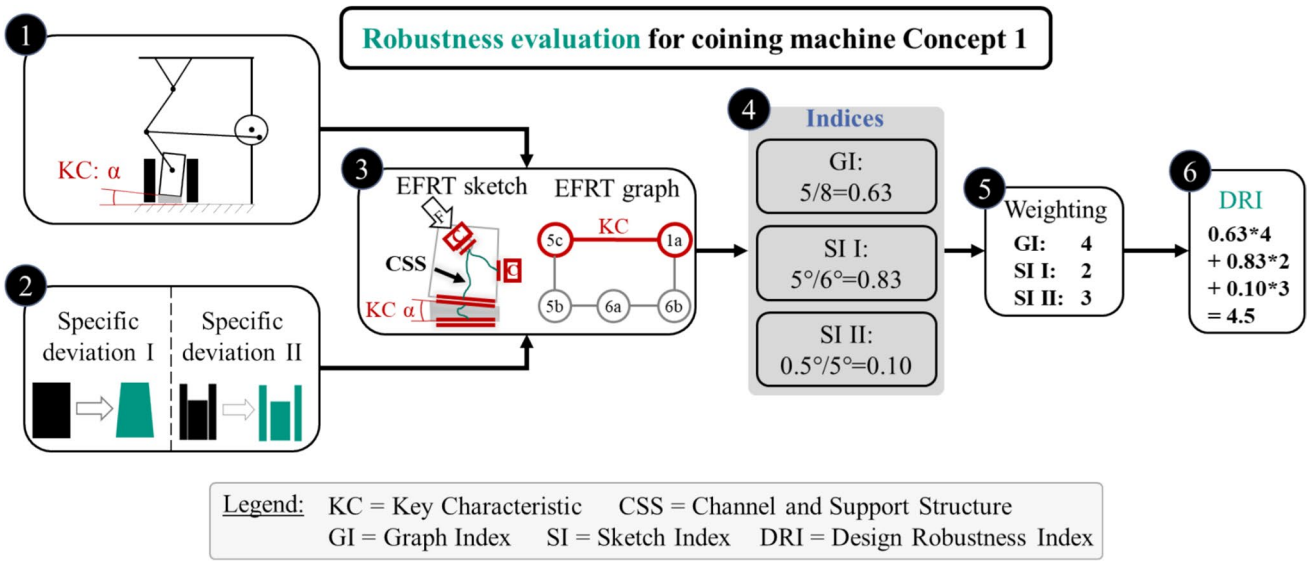

Fig. 7 Application of the six-step EFRT-based method for robustness evaluation to Concept 1 of the coining machine, resulting in the Design Robustness Index

accuracy. Scaling the deviation magnitudes would not affect the qualitative behavior or the relative robustness ranking of the investigated concepts.

In Step 3, the EFRT graphs and EFRT sketches were derived. State modeling was carried out for piston shape deviation and clearance deviation across all 16 concepts, resulting in a total of 32 EFRT sketches. Since the EFRT graph does not consider specific geometric deviations, each concept is represented by only one EFRT graph. Concepts 1–8, due to their identical system structure, share the same EFRT graph. In contrast, due to differences in the connection of the guide mechanism to the frame, Concepts 9–16 are characterized by a distinct EFRT graph.

In Step 4, the Graph Indices and Sketch Indices were determined. For the EFRT graph, concepts 1–8 had five GEs, as shown in Fig. 7, while Concepts 9–16 included eight GEs in their EFRT graph (see Fig. 8 Concept 9). Using Eq. (1), the Graph Indices could be calculated. For the EFRT sketches, state modeling for the minting state was performed, including piston shape deviation and clearance

Concept	Concept 3			Concept 5		
EFRT modeling	**EFRT sketch I** for deviation I	**EFRT sketch II** for deviation II	**EFRT graph** for general deviations	**EFRT sketch I** for deviation I	**EFRT sketch II** for deviation II	**EFRT graph** for general deviations
Indices	SI_1=3°/6°=0.50	SI_2=0.5°/5°=0.10	GI=5/8=0.63	SI_1=2°/6°=0.33	SI_2=0.5°/5°=0.10	GI=5/8=0.63
Weighting	2	3	4	2	3	4
DRI	**3.8**			**3.5**		

Concept	Concept 9			Concept 10		
EFRT modeling	**EFRT sketch I** for deviation I	**EFRT sketch II** for deviation II	**EFRT graph** for general deviations	**EFRT sketch I** for deviation I	**EFRT sketch II** for deviation II	**EFRT graph** for general deviations
Indices	SI_1=5°/6°=0.83	SI_2=0.5°/5°=0.10	GI=8/8=1.00	SI_1=6°/6°=1.00	SI_2=5°/5°=1.00	GI=8/8=1.00
Weighting	2	3	4	2	3	4
DRI	**6.0**			**9.0**		

Legend: KC = Key Characteristic CSS = Channel and Support Structure
GI = Graph Index SI = Sketch Index DRI = Design Robustness Index

Fig. 8 Excerpt from the results of the robustness evaluation. Low DRI means higher robustness. Concept 5 is the most robust of the four presented concepts, whereas Concept 10 demonstrated the lowest robustness

deviation. This allowed the evaluation of the deviation in KC. i.e., the coin angle, for each concept during this state. The Sketch Index was then calculated using Eq. (2), based on the maximum evaluated coin angle throughout the concepts and the evaluated angle in the current concept. For instance, as illustrated in Fig. 7, the EFRT sketch for Concept 1 showed that due to the tilting moment, the piston consistently contacted the guide during the minting process. Consequently, the KC angle was evaluated to be 5°, reflecting the 5° piston shape deviation.

In Step 5, the weighting factors for the Graph Indices and Sketch Indices were defined (see Fig. 7). Based on experience gained from the manufacturing and testing of the previous generation of coining machines, the following weighting factors were assigned: the Graph Index received a weighting factor of 4, as the "very coarse" tolerance class was selected according to ISO 2768–1. The Sketch Index for piston shape deviation was given a weighting factor of 2, considering the small probability of occurrence in typical operational conditions. The Sketch Index for clearance deviation was assigned a weighting factor of 3, reflecting its relatively higher likelihood of this deviation occurring due to common manufacturing inaccuracies.

In Step 6, the indices of all the concepts were summed up to derive the DRI using Eq. (3). Due to the scope of this paper, this section presents selected examples of the results (see Fig. 8). The full results of the robustness evaluation, encompassing all 16 DRIs, have been published as research data for further reference (Li et al. 2024a).

As described earlier, design decisions regarding four different design characteristics must be made. All of these characteristics can be seen in the selected examples (see Fig. 8). The borehole position differs in Concept 3 compared to the other concepts. The connecting rod length in Concept 5 is shorter than in the other concepts. The guide length in Concept 10 is shorter than in the other concepts. The guide connection in Concept 3 and Concept 5 differs from those in Concept 9 and Concept 10.

As shown in Fig. 8, the system structures of the concepts differed, resulting in two distinct EFRT graphs across the concepts. Concepts 1–8 featured 5 GEs in their EFRT graphs, while Concepts 9–16 had 8 GEs. Consequently, Concepts 3 and 5 received a Graph Index of 5/8 = 0,625, while Concept 9 and 10 had a Graph Index of 8/8 = 1.

Using EFRT sketches, the KC values for the example concepts were evaluated regarding piston shape deviation. In Concept 9, the tilting moment caused the piston's right edge to rest against the guide during the coining state, leading to an estimated KC of 5° (see Fig. 8 EFRT sketch I). For Concept 3, the tilting moment was smaller due to the reduced lever arm. The resistance during the coining state caused the piston to re-center, and the KC value was estimated at 3°. In Concept 5, the relatively perpendicular force application led to the piston re-centering against the coin's resistance. This smaller transverse force component in Concept 5 suggested that the tilting moment in Concept 5 was lower than in Concept 3, resulting in an estimated KC of 2°. For Concept 10, the maximum KC value of 6° was evaluated, as the tilting moment and short guide caused further tilting of the piston. The Sketch Indices for the piston shape deviations were then calculated. Concept 3 received a Sketch Index of 3°/6° = 0.5, Concept 5 received 2°/6° = 0.33, Concept 9 received 5°/6° = 0.83 and Concept 10 received 6°/6° = 1.

Regarding clearance deviation, the KC values for the example concepts were evaluated using different EFRT sketches resulting from the state modeling. In Concepts 3, 5, and 9, due to the force application direction, the piston is pressed against the right side of the guide, ensuring optimal guidance. Consequently, a KC value of 0.5° was estimated, reflecting only the general tolerance. For Concept 10, the transverse force component caused the piston to tilt, forming contact pairs at the upper right and lower left of the guide. The tilt is limited by the clearance between the piston and the guide, and with increased clearance, a KC of 5° was estimated. The maximum KC value among all concepts caused by clearance deviation was determined to be 5°, also occurring in Concept 10. Thus, the Sketch Indices for clearance deviation were calculated as follows: Concept 3, 5 and 9 had a Sketch Index of 0.5°/5° = 0.1, while Concept 10 had a Sketch Index of 5°/5° = 1.

Using a weighting factor defined in Step 5, the DRIs were calculated as shown in Fig. 8. Concept 5 was evaluated as the most robust among the example concepts, whereas Concept 10 demonstrated the lowest robustness. It is important to emphasize that this evaluation is based on analysis using physical laws, which necessitates certain assumptions during the process. While state modeling supports these estimations, it does not guarantee their accuracy. To address this, additional testing activities are carried out in this paper to determine the reliability of the findings.

4.2 Validation of the robustness evaluation through testing

In the early stages of development, no fully developed CAD models are available as a basis for gaining knowledge through simulative or physical testing. To gain the necessary knowledge, surrogate models are used to make the testing through an early simulation and prototype possible. The key requirement for these surrogate models is that they must have suitable fidelity, meaning they should exhibit similar physical behavior to the real product for the intended purpose. Given that the coining machine is not a highly dynamic system, the focus of the validation lies in the kinematic states. The surrogate models of the evaluated

concepts will be prepared for validation through experiments or simulations.

As presented in Sect. 2.1, there are case distinctions in the robustness evaluation depending on whether system states are known or require further analysis to determine. This also results in case distinctions during the validation process. The Graph Index evaluates the system structure under the assumption that the geometric deviation remains within the general tolerance limits and no additional degrees of freedom are introduced. In this case, the boundary conditions for the simulation with a simplified CAD model can be defined. Simulations can efficiently handle a large number of samples to show the impact of general geometric deviations on KC, an advantage that is often impractical to achieve through physical experimentation. Therefore, an early simulation is suitable for validating the Graph Index, allowing the effect of different system structures on robustness to be demonstrated.

As the piston shape deviation and the clearance deviation can lead to additional degrees of freedom in the coining machine, state modeling becomes essential for examining the system's behavior under each deviation. To validate the state modeling under these specific deviations and the resulting Sketch Indices, physical experiments are considered appropriate. These specific deviations often have a primary impact on the KC, making them suitable for investigation through targeted individual experiments. For these experiments, we use rapid prototyping techniques to obtain quick results.

4.2.1 Validation of the Graph Index using simulation

Concerning the design characteristic "guide connection," two distinct EFRT graphs are generated, representing two different Graph Indices across all concepts. The indices differ between Concepts 1–8, where the guide is connected to the bed, and Concepts 9–16, where the guide is attached to the frame. Concepts 1 and Concept 9 are selected as examples for the simulation study.

To validate the two Graph Indices, we conducted simulations using a two-dimensional variation simulation software. The simulation follows the root sum square (RSS) method. A minor angular deviation from a rectangle ($\pm 2°$, normally distributed) was introduced at each connection point in the system to observe its impact on the KC across the different concepts (see Fig. 9). These connection points are also represented in the EFRT graphs. Rejection was defined as cases where the KC value exceeded $\pm 2°$, with the rejection rate expressed in parts per million (ppm). The KC distributions for Concept 1 and Concept 9 are compared to validate their robustness due to varying system structures.

The Graph Indices and the simulation results for Concepts 1 and 9 are presented in Fig. 9. On the left, the EFRT graphs and Graph Indices show that Concept 1, with a lower Graph Index, is more robust than Concept 9, as detailed in Sect. 4.1. The simulation results are illustrated on the right: the x-axis represents KC values, while the y-axis displays the number of samples for each KC value. Red lines indicate the KC limits, and the dashed line represents the target

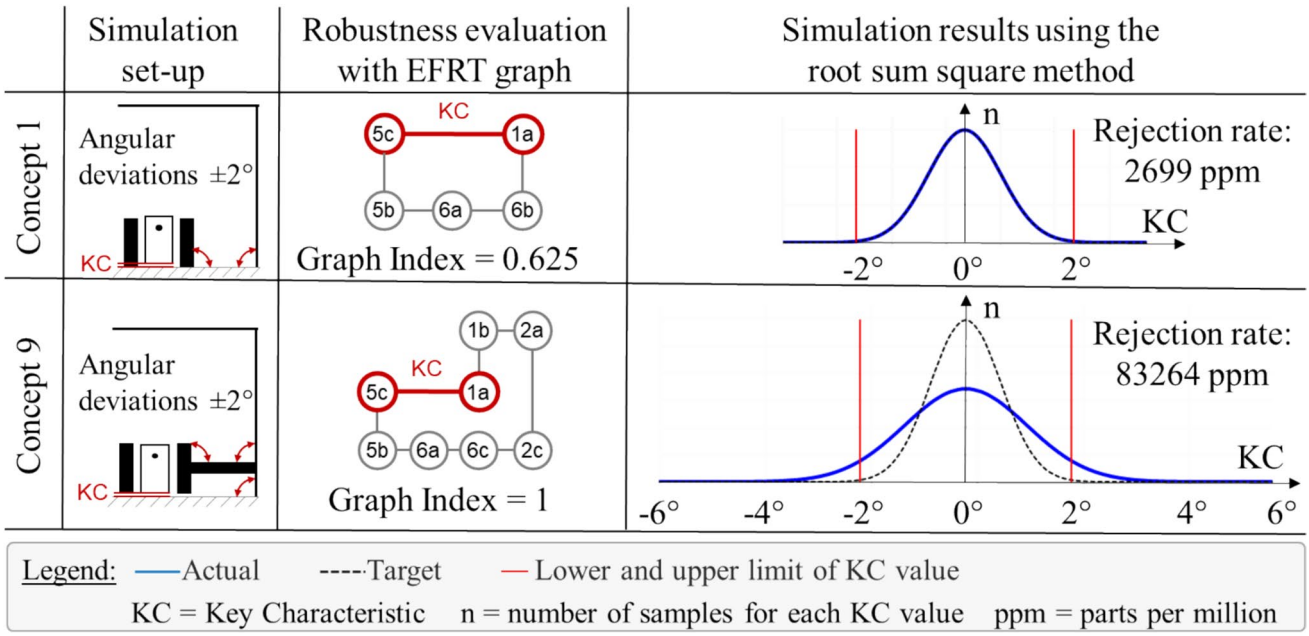

Fig. 9 Validation of Graph Indices using simulation results. Concept 1 demonstrates higher robustness than Concept 9, as indicated by a higher Graph Index, which aligns with the findings from the simulation

KC distribution (with the majority of KC values within 6σ). The blue curve depicts the actual KC distribution. For Concept 1, the blue and dashed lines align. A low rejection rate (2699 ppm) can be observed. In contrast, the distribution of KC value in Concept 9 is much wider, with many samples exceeding the limits, leading to a significantly higher rejection rate (83,264 ppm). This discrepancy is due to the fact that Concept 1 has fewer contributors to KC due to its system structure, making it less sensitive to other geometric deviations compared to Concept 9.

4.2.2 Validation of the Sketch Index using experiment

To validate the state modeling of the EFRT sketch, physical tests are required to capture the real behavior of the coining machine. This process can be seen in Fig. 10. First, a test environment was created to enable testing. This environment will define the test plan, surrogate models, prototype manufacturing method, and the measurement and analysis process. Since the state modeling for Concepts 1–8 does not differ from Concepts 9–16, the tests are only conducted for Concepts 1–8 to avoid duplication. CAD surrogate models with and without specific deviations were created. 24 tests were conducted, eight each for clearance deviation, piston deviation, and ideal geometry. The piston shape deviation was modeled by a 5° tilt between the piston bottom edge and side edge, and the clearance deviation was simulated by extending the guide width by 2 mm. High-density fiberboard was used for manufacturing the prototypes, which were manufactured using a laser cutting machine. A modeling compound was selected for the coin material, as it deforms primarily in a plastic manner. Before testing, the coin material was cut into uniform pieces and placed into the coining machine for minting. Figure 10 on the left shows the coining machine prototypes with the design characteristic borehole position (top and bottom). In this example, piston shape deviation was also introduced. To ensure better comparability of the results, the initial testing phase was conducted using coining machines produced based on the ideal CAD model. Relevant components exhibiting shape deviations and concept modifications were subsequently replaced within the coining machine during testing.

For measurement, the minted coins were fixed in a camera stand after testing and photographed (see Fig. 10 in the middle). By fixing the test object and camera lens, measurement repeatability can be ensured to gather reliable data. The KC value, i.e., the angle of the coin, was measured graphically from the photos (see Fig. 10 on the right). To minimize measurement errors and exclude outliers, each test was repeated three times, and the median value was taken.

Table 1 presents the results of the experiments for the different concepts. In the second column, the angular measurements of the key characteristic for the ideal geometry in the CAD model are shown, where manufacturing-dependent

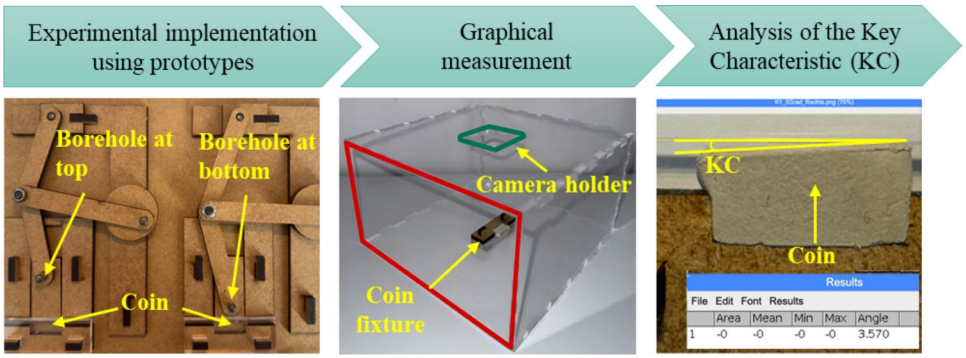

Fig. 10 Experimental workflow for measuring the key characteristic (KC) using coining machine prototypes. In this example, prototypes with different borehole positions are implemented (left); the coin angle is recorded by graphical measurement using a fixed camera setup (middle); and the key characteristic is quantitatively analyzed from the measurement results (right)

Table 1 Measured coin angles from the experiments for different concepts and deviations

Concept	Measured coin angle by ideal CAD geometry	Measured coin angle by Piston shape deviation 5°	Measured coin angle by Clearance deviation 2 mm
1	0.68°	4.50°	0.67°
2	0.92°	5.08°	6.53°
3	0.64°	3.68°	0.88°
4	0.59°	3.57°	1.07°
5	0.35°	3.81°	1.08°
6	1.47°	6.11°	1.65°
7	0.41°	2.78°	0.91°
8	0.37°	3.80°	0.98°

deviations are present. This highlights the impact of general tolerances on functional fulfillment. The experimental results for piston shape deviation and clearance deviation are shown in columns three and four.

4.3 Evaluation of the case study

The evaluation of the case study focused on the experimental results, as the alignment between the Graph Index and simulation results was already discussed in Sect. 4.2.1. The results from both the robustness evaluation and the experiments are summarized and compared in Fig. 11. For better comparison, the measured angles were normalized. The largest measured angle across all concepts under a given deviation was used as the denominator, while the actual measured angles in the current concept were used as the numerator. This allows for comparing the Sketch Indices with the normalized measured KC values. By comparing these results, partial validation of the Sketch Indices is achieved. While the case study shows a general alignment between the robustness evaluation and the validation results, some discrepancies indicate that not all indices could be fully validated. The results show that while the proposed method is promising, further investigation is necessary to enhance its reliability.

This evaluation relies on analysis using physical laws, requiring certain assumptions. While the EFRT-based method supports these estimations, further testing is needed to confirm the accuracy of the assumptions. For example, the robustness evaluation for Concepts 3 and 5 regarding piston shape deviation did not align with the testing results (see Fig. 11). This highlights the need for a deeper investigation into the differences between the robustness evaluation and the validation study. According to the robustness evaluation, Concept 5 was expected to be more robust than Concept 3, as a smaller angle was predicted by the state modeling. However, the experimental results show that the angle between Concepts 3 and 5 did not differ significantly. This discrepancy can be attributed to incorrect assumptions made during the evaluation. Specifically, the tilting moment is a product of the force component and the lever arm. The assumption made during the robustness evaluation was that the force component would have a greater impact on the tilting moment, causing the piston in Concept 3 to tilt more than in Concept 5. In contrast, the experimental results revealed that the tilting moment in Concept 3, due to its shorter lever arm, was on a similar level to that of Concept 5, leading to similar angular deviations in both concepts. This suggests that to achieve a reliable robustness evaluation, some insights must be tested early on. Therefore, it is valuable to integrate robustness evaluation with experimental testing to gain more accurate insights into the robustness.

The case study also demonstrated that the Sketch Index has to be calculated separately for each specific deviation. In Concept 9, the piston is pressed against the guide due to the force input, which has a different impact on the KC. For the piston shape deviation, a larger deviation in KC is expected. In contrast, for clearance deviation, the piston is not tilted, and it is beneficial when the piston is in contact with the guide, as it results in better guidance and a smaller KC. To achieve a more robust evaluation, it is crucial to consider both these differences in the effect analysis with state modeling, as well as their respective weightings in the overall evaluation.

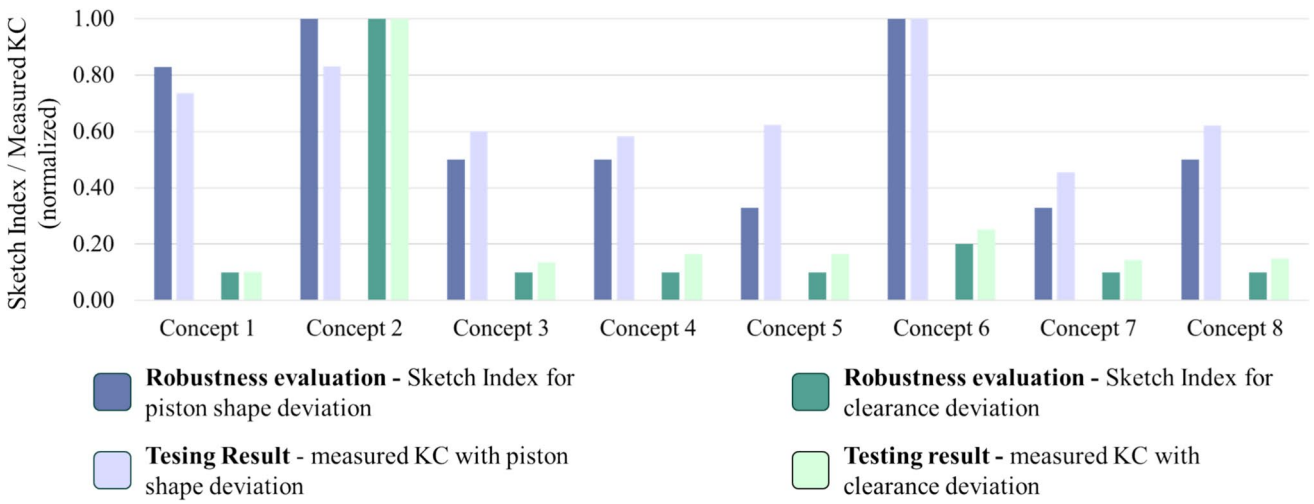

Fig. 11 Validation of the Sketch Indices by comparing the Sketch Indices from robustness evaluation with normalized measured key characteristic (KC) values obtained from testing, for piston shape and clearance deviations across eight design concepts

5 Discussion

Based on the case study results, the research question *"How can the robustness of product concepts against geometric deviations in the early stages of product development be quantitatively evaluated?"* can be answered as follows.

This research addresses a key gap identified in Sect. 2.2, which is the lack of methods that quantitatively assess the robustness of product concepts by simultaneously considering both geometric structures and the functional behavior of the product concept. This gap is addressed by the proposed EFRT-based method, which systematically evaluates how different geometric deviations impact functional fulfillment. The DRI is systematically derived in a six-step process and used to compare the robustness of different product concepts, providing a quantitative foundation for early-stage decision-making in the design process.

Using the EFRT-based method, it is possible to conduct a well-founded robustness evaluation in the early stages of product development. Compared to traditional methods that rely on experiments or simulations conducted at later stages with well-defined geometry (Qin et al. 2017; Taguchi et al. 2005), robustness evaluation can be performed analytically at an earlier stage, facilitating the exploration of robust preliminary geometries and parameter spaces with fewer resources. By making appropriate assumptions about system states, initial insights into the robustness of product concepts can be obtained. These insights can later be validated and refined through traditional methods. Consequently, the EFRT-based method enhances system understanding and supports decision-making in design by creating insightful mental models.

The EFRT-based method can extend existing early RD methods introduced in the state of the art. While critical geometric deviations can be identified using methods such as VMEA (Johansson et al. 2006), the proposed method goes further by evaluating of the impact of these deviations on the functional fulfillment of various design decisions. The new insights gained through this method support the effective use of existing RD principles (Andersson 1997; Ebro and Howard 2016; Eifler and Howard 2017) by allowing the effects of these principles to be modeled for individual product concepts. The criterion used to evaluate the Graph Index is consistent with the RD principle of load path shortening (Li et al. 2023), an established principle for reducing the number of contributors to a KC, while EFRT modeling assists in identifying effective load paths. In later design stages, robustness is determined by the magnitude and propagation of uncertainties rather than by the number of influencing factors alone. The proposed Graph Index therefore serves as an early-phase heuristic and should not be interpreted as a substitute for detailed tolerance or uncertainty analysis. Other principles, such as the avoidance of coupling (Goetz 2024), could also be used to evaluate the Graph Index though this introduces additional complexity and its integration as an evaluation criterion requires further investigation. Furthermore, while the graph-based method proposed by Goetz et al. (2019), which considers the general geometric deviations, has been integrated into the EFRT-based method, more insights can be gained into undefined system states caused by specific geometric deviations. This is particularly evident in Concept 3, 5 and 9 (see Fig. 8), where piston shape deviation and clearance deviation result in different Sketch Indices with an unchanged EFRT graph.

Classical approaches supporting mechanism design, such as kinematic or variation simulations, require fully specified geometry, parameters, and boundary conditions and are therefore primarily suited to later, detailed design stages. In early conceptual phases, this information is typically unavailable, and generating it requires substantial additional modeling effort. While such simulations can, in principle, also be applied to the mechanisms studied in this work, their use here is limited to validation purposes, as demonstrated by the variation simulation conducted in Sect. 4.2.1 to assess the variation of the KC. The objective of this work is not to replace established kinematic or variation simulations, but to complement them by enabling robustness evaluation at an early design stage, when detailed models are not yet available. At this stage, design engineers primarily focus on system structure and expected system behavior rather than on fully parameterized kinematic simulations. The proposed DRI derived from Eq. (3) does not rely on explicitly defined design parameters. Instead, it evaluates differences in system structure and behavior through EFRT graphs and sketches, making it particularly suitable for early-stage robustness assessment.

The EFRT-based method uses KC, often a geometric measure, as an indicator of functional performance. However, in highly dynamic systems, functional fulfillment is frequently assessed using other physical parameters, such as vibrations. In such cases, it is necessary to identify relevant geometric measures through their physical relationships, as demonstrated by Li et al. (2024d). While this paper shows a case study using a single KC, systems with multiple KCs or areas of interest require the calculation of additional Graph Indices and Sketch Indices. These indices must also be appropriately weighted to provide a comprehensive evaluation. Different strategies, such as those proposed by Goetz et al. (2020) or Juul-Nyholm and Eifler (2024), can provide insights into assigning weights based on factors like occurrence probability and importance. While it is inherently challenging to guarantee complete and accurate identification of all KCs and geometric deviations, the structured modeling method enhances the comprehensiveness of this

identification process. By embedding expert knowledge and experience-driven parameter selection within the method, critical factors can be systematically incorporated, although some degree of subjectivity remains unavoidable.

The proposed method is tailored to specific stages within the product development process, aligning with its intended application boundaries. Specifically, the EFRT-based method is not designed for the ideation phase, where the primary focus is on generating broad and creative concepts. Instead, it is better suited for subsequent stages, where the robustness of preliminary geometric features is analyzed and evaluated. The method's effectiveness depends on having concepts with adequate maturity that enable meaningful and reliable comparisons. The application of this method is still in the early stages of product development, as detailed parameterization has not yet been fully implemented. Although the EFRT-based method evaluates different deviations separately, it does not consider their interactions. This limitation is due to the increased complexity of interaction effects, which are challenging to estimate during the design phase. In addition, determining the Sketch Index involves subjective assessment and relies on the design engineer's design knowledge. While the EFRT-based method provides guidance for this determination, it carries a certain risk of misjudgment due to incorrect assumptions or limited knowledge. Early-stage testing can mitigate this uncertainty by providing empirical data to validate or adjust these subjective assessments, thereby increasing the reliability of the robustness evaluation.

Following the recommendations of Blessing and Chakrabarti (2009), an initial validation of the proposed method was conducted through a case study involving a coining machine. Section 4 not only demonstrates the application of the method but also presents an evaluation supported by experimental data. This provides the readers with a transparent and practical illustration of the method's use within the presented case study and offers guidance for its transferability to other systems. The evaluation of design methods is essential for their acceptance in industry and for their ongoing development (Cash 2018; Gericke et al. 2017). Further case studies in industrial settings are necessary to comprehensively validate the method's applicability and generalizability across diverse systems and user contexts.

The determination of weighting factors for the Graph Index and Sketch Index requires expert judgment and domain-specific knowledge. While the proposed four-point Likert scale provides a structured and transparent framework for assigning these weights, the resulting values remain context-dependent and organization-specific. Consequently, the weighting factors should be interpreted as calibrated assessments rather than objective constants. Future work will investigate the inter-rater reliability, calibration, and acceptance of the proposed weighting scheme through empirical user studies involving design engineers from different organizational contexts.

The limitations of the validation study are related to the fidelity of the surrogate model, which was created using initially estimated parameters and does not fully reflect the actual 3D assembly, with many details intentionally omitted. It should be noted that the prototype's purpose is not to precisely simulate the detailed real deviations found in finished industrial products. Instead, the focus lies in investigating the influence of critical geometric deviations on functional behavior early in the design process. Additionally, measurement errors are unavoidable with the measurement technique used. However, these errors are acceptable given the scale of the geometric deviations under consideration. The surrogate models used in this study are considered adequate for validating the state modeling and assessing the effects of geometric deviations.

6 Conclusion and outlook

This paper has presented the EFRT-based method for robustness evaluation, which facilitates the quantitative evaluation of product concepts' robustness against geometric deviations. The relationship between geometric deviations and functional fulfillment was modeled using the EFRT-based method, with the EFRT sketch and graph evaluating the impact of deviations on KCs. From this evaluation, the Graph Index and Sketch Index were derived. A subsequent weighting process facilitated the calculation of the DRI, allowing a comparative analysis of the robustness of various product concepts. The method was applied in a case study involving a coining machine. The indices were validated through simulations and experiments using surrogate models. The case-study results demonstrated good agreement between the theoretical robustness evaluation through the EFRT-based method and the testing results. Consequently, the proposed method provides design engineers with a solid foundation for evaluating the robustness of product concepts and making well-informed decisions. By evaluating the impact of geometric deviations on a product concept's functional fulfillment in the early stages, this method minimizes the risk of costly design iterations and contributes to the design of more robust and reliable products.

The validation study in this paper was conducted by the authors themselves, comparing the results of the robustness evaluation with empirical testing. This initial validation focuses solely on the robustness evaluation and does not address the applicability of the method by other users. Future research could explore whether similar results emerge if the robustness evaluation is performed by other design engineers in a subject study. Investigating the

method within an industrial context is also crucial, as this would help assess the benefits of the method in practical design environments. Additionally, applying other state-of-the-art robustness evaluation methods within a subject study could offer valuable comparisons and highlight differences among the methods.

While the proposed method supports design engineers in robustness evaluation, the process remains manual and cognitively demanding. Future work could explore partial automation of this evaluation using data-driven approaches. For example, relations between geometric deviations and functional behavior, as represented in EFRT sketches, could be transformed into structured textual design hypotheses. These hypotheses could then be used to train large language models to generate a knowledge database, enhancing efficiency in decision-making.

Acknowledgements This work was funded by the Deutsche Forschungsgemeinschaft (DFG, German Research Foundation) within the project "Holistic robustness evaluation in early design stages" under grant number 467789897. The support is gratefully acknowledged.

Author contributions Li wrote the main manuscript text and contributed to method development and the study design for the case study. Horber contributed to method development and performed the simulations. Demir conducted the experiments. Renner contributed to the robustness evaluation in the case study. Grauberger, Goetz, Wartzack, and Matthiesen provided input for the method development. All authors reviewed the manuscript.

Funding Open Access funding enabled and organized by Projekt DEAL.

Data availability The complete research data has been published and is available for further reference at: https://doi.org/10.5445/IR/1000177592.

Declarations

Conflict of interest The authors have no competing interests to declare that are relevant to the content of this article.

References

Al Handawi K, Brahma A, Wynn DC, Kokkolaras M, Isaksson O (2024) Design space exploration and evaluation using margin-based trade-offs. J Mech des 146:061701. https://doi.org/10.1115/1.4063966

Albers A, Rapp S (2022) Model of SGE: system generation engineering as basis for structured planning and management of development. In: Krause D, Heyden E (eds) Design methodology for future products. Springer International Publishing, Cham, pp 27–46

Andersson P (1997) On robust design in the conceptual design phase: a qualitative approach. J Eng des 8:75–89. https://doi.org/10.1080/09544829708907953

Andreasen MM, Hansen CT, Cash P (2015) Conceptual design: interpretations, mindset and models. Springer International Publishing, Cham

Arvidsson M, Gremyr I (2008) Principles of robust design methodology. Qual Reliab Eng Int 24:23–35. https://doi.org/10.1002/qre.864

Blessing LTM, Chakrabarti A (2009) DRM, a design research methodology. Springer, London. https://doi.org/10.1007/978-1-84882-587-1

Brahma A, Wynn DC (2020) Margin value method for engineering design improvement. Res Eng Design 31:353–381. https://doi.org/10.1007/s00163-020-00335-8

Brahma A, Wynn DC, Isaksson O (2022) Use of margin to absorb variation in design specifications: an analysis using the margin value method. Proc des Soc 2:323–332. https://doi.org/10.1017/pds.2022.34

Brix T, Husung S, Döring U (2025) Strategies and methods for robust design in the early phases of product development in precision engineering. In: 3rd international conference on advanced mechanism and machine technology. https://doi.org/10.22032/dbt.64949

Brown T (2008) Design thinking. Harv Bus Rev 86:84

Cash PJ (2018) Developing theory-driven design research. Des Stud 56:84–119. https://doi.org/10.1016/j.destud.2018.03.002

Ebro M, Howard TJ (2016) Robust design principles for reducing variation in functional performance. J Eng des 27:75–92. https://doi.org/10.1080/09544828.2015.1103844

Eifler T, Howard TJ (2017) Exact constraint design and its potential for robust embodiment. Procedia CIRP 60:302–307. https://doi.org/10.1016/j.procir.2017.02.046

Eifler T, Howard TJ (2018) The importance of robust design methodology: case study of the infamous GM ignition switch recall. Res Eng des 29:39–53. https://doi.org/10.1007/s00163-017-0251-x

Eifler T, Schleich B (2021) A robust design research landscape—review on the importance of design research for achieving product robustness. Proc des Soc 1:211–220. https://doi.org/10.1017/pds.2021.22

Eppinger SD, Whitney DE, Smith RP, Gebala DA (1994) A model-based method for organizing tasks in product development. Res Eng des 6:1–13. https://doi.org/10.1007/BF01588087

Faheem F, Li Z, Husung S (2023) Analysis of potential errors in technical products by combining knowledge graphs with MBSE approach. https://doi.org/10.22032/dbt.58898

Geis A, Husung S, Oberänder A, Weber C, Adam J (2015) Use of vectorial tolerances for direct representation and analysis in CAD-systems. Procedia CIRP 27:230–240

Gericke K, Eckert C, Stacey M (2017) What do we need to say about a design method. In: Proceedings of the 21st international conference on engineering design. ICED'17, Vancouver, Canada, pp 101–110

Gero JS, Kannengiesser U (2014) The function-behaviour-structure ontology of design. In: Chakrabarti A, Blessing LTM (eds) An anthology of theories and models of design: philosophy, approaches and empirical explorations. Springer, London, pp 263–283

Goetz S (2024) Early tolerance management and robust design. In: Wartzack S (ed) Research in tolerancing. Springer Nature Switzerland, Cham, pp 39–62

Goetz S, Schleich B, Wartzack S (2018) A new approach to first tolerance evaluations in the conceptual design stage based on tolerance graphs. Procedia CIRP 75:167–172. https://doi.org/10.1016/j.procir.2018.04.030

Goetz S, Hartung J, Schleich B, Wartzack S (2019) Robustness evaluation of product concepts based on function structures. Proc Int Conf Eng des 1:3521–3530. https://doi.org/10.1017/dsi.2019.359

Goetz S, Schleich B, Wartzack S (2020) Integration of robust and tolerance design in early stages of the product development process. Res Eng des. https://doi.org/10.1007/s00163-019-00328-2

Göhler SM, Howard TJ (2015) The contradiction index (CI): a new metric combining system complexity and robustness for early design stages. In: 27th International conference on design theory and methodology, Boston, Massachusetts, USA. 2015. https://doi.org/10.1115/DETC2015-47255

Gremyr I, Hasenkamp T (2011) Practices of robust design methodology in practice. TQM J 23:47–58. https://doi.org/10.1108/17542731111097489

Hasenkamp T, Arvidsson M, Gremyr I (2009) A review of practices for robust design methodology. J Eng des 20:645–657. https://doi.org/10.1080/09544820802275557

Hatcher G, Ion W, Maclachlan R, Marlow M, Simpson B, Wilson N, Wodehouse A (2018) Using linkography to compare creative methods for group ideation. Des Stud 58:127–152. https://doi.org/10.1016/j.destud.2018.05.002

Horber D, Li J, Grauberger P, Schleich B, Matthiesen S, Wartzack S (2022) A model-based approach for early robustness evaluation—combination of contact and channel approach with tolerance graphs in SysML. In: Proceedings of the 33rd symposium design for X. DFX 2022, Hamburg. https://doi.org/10.35199/dfx2022.18

Horber D, Li J, Grauberger P, Goetz S, Matthiesen S, Wartzack S (2024) Robust conceptual design for a robust early embodiment design. In: Proceedings of NordDesign 2024. NordDesign 2024, Reykjavik, Iceland, 12th–14th August 2024. The Design Society, pp 11–20. https://doi.org/10.35199/NORDDESIGN2024.2

Johansson P, Chakhunashvili A, Barone S, Bergman B (2006) Variation mode and effect analysis: a practical tool for quality improvement. Qual Reliab Engng Int 22:865–876. https://doi.org/10.1002/qre.773

Jugulum R, Frey DD (2007) Toward a taxonomy of concept designs for improved robustness. J Eng des 18:139–156. https://doi.org/10.1080/09544820600731496

Juul-Nyholm HK, Eifler T (2024) Multi-objective robustness indicators for evaluation and exploration of design margins. J Eng des 35:1227–1257. https://doi.org/10.1080/09544828.2023.2261336

Kleinhans L, Li J, Grauberger P, Matthiesen S (2024) Incorporating tolerances into qualitative reliability models. In: DS 133: Proceedings of the 35th symposium design for X (DFX2024). The Design Society, pp 182–191. https://doi.org/10.35199/dfx2024.19

Li J, Horber D, Keller C, Grauberger P, Goetz S, Wartzack S, Matthiesen S (2023) Utilizing the embodiment function relation and tolerance model for robust concept design. In: Proceedings of the design society 2023, vol 3, pp 3771–3780. https://doi.org/10.1017/pds.2023.378

Li J, Demir F, Renner P, Grauberger P, Matthiesen S (2024a) Design robustness index for evaluating the robustness of product concept. KIT Scientific Working Papers 255, Karlsruhe. https://doi.org/10.5445/IR/1000177592

Li J, Horber D, Grauberger P, Goetz S, Wartzack S, Matthiesen S (2024b) Supporting early robust design for different levels of specific design knowledge: an adaptive method for modeling with the Embodiment Function Relation and Tolerance Model. Des Sci 10:e46. https://doi.org/10.1017/dsj.2024.48

Li J, Horber D, Renner P, Yan J, Goetz S, Grauberger P, Wartzack S, Matthiesen S (2024c) Investigating modeling in early robust design – a study with the modeling method of embodiment function relation and tolerance model. In: Proceedings of NordDesign 2024. NordDesign 2024, Reykjavik, Iceland, 12th–14th August 2024. The Design Society, pp 133–142. https://doi.org/10.35199/NORDDESIGN2024.15

Li J, Long Y, Döllken M, Zhang Y, Wu G, Matthiesen S(2024d) Linking early robust design with quantitative methods for enhanced industrial applications. In: Volume 1: Acoustics, vibration, and phononics; advanced design and information technologies. ASME 2024 international mechanical engineering congress and exposition, Portland, Oregon, USA. 17.11.2024–21.11.2024. American Society of Mechanical Engineers. https://doi.org/10.1115/IMECE2024-144707

Mathias J, Kloberdanz H, Eifler T, Engelhardt R, Wiebel M, Birkhofer H, Bohn A (2011) Selection of physical effects based on disturbances and robustness ratios in the early phases of robust design. In: Proceedings of the 18th international conference on engineering design. ICED'11, Lyngby/Copenhagen, Denmark, pp 324–335

Matthiesen S, Grauberger P, Schrempp L (2019) Extended sequence modelling in design engineering—gaining and documenting knowledge about embodiment function relations with the C&C^2-approach. In: Proceedings of the 22nd international conference on engineering design, ICED19. Delft, The Netherlands

Morse E, Dantan J-Y, Anwer N, Söderberg R, Moroni G, Qureshi A, Jiang X, Mathieu L (2018) Tolerancing: managing uncertainty from conceptual design to final product. CIRP Ann 67:695–717

Müller JR, Isaksson O, Landahl J, Raja V, Panarotto M, Levandowski C, Raudberget D (2019) Enhanced function-means modeling supporting design space exploration. AI EDAM 33:502–516. https://doi.org/10.1017/S0890060419000271

Pahl G, Beitz W, Feldhusen J, Grote K-H (2007) Engineering design: a systematic approach, 3rd edn. Springer, London, p 617

Petersson AM, Lundberg J (2018) Developing an ideation method to be used in cross-functional inter-organizational teams by means of action design research. Res Eng des 29:433–457. https://doi.org/10.1007/s00163-018-0283-x

Phadke MS (1989) Quality engineering using design of experiments. In: Dehnad K (ed) Quality control, robust design, and the taguchi method. Springer, Boston, pp 31–50

Qin Y, Qi Q, Lu W, Liu X, Scott PJ, Jiang X (2017) A review of representation models of tolerance information. Int J Adv Manuf Technol 2:156. https://doi.org/10.1007/s00170-017-1352-4

Robbins N, Heiberger R (2011) Plotting Likert and other rating scales. In: Proceedings of the 2011 joint statistical meeting, Miami, USA. American Statistical Association, pp 1058–1066

Suh NP (1998) Axiomatic design theory for systems. Res Eng des 10:189–209. https://doi.org/10.1007/s001639870001

Taguchi G, Chowdhury S, Wu Y, Taguchi S, Yano H (2005) Taguchi's quality engineering handbook. Wiley, Hoboken, Livonia

Thornton A (2004) Variation risk management: Focusing quality improvements in product development and production. Wiley, Hoboken, p 320

Thunnissen DP, Tsuyuki GT (2004) Margin determination in the design and development of a thermal control system. In: SAE technical paper series. International conference on environmental systems. JUL. 19, 2004. SAE International 400 Commonwealth Drive, Warrendale, PA, United States. https://doi.org/10.4271/2004-01-2416

Ullman DG (2010) The mechanical design process, 4th edn. McGraw-Hill Higher Education, New York, p 433

Weber C (2014) Modelling products and product development based on characteristics and properties. In: Chakrabarti A, Blessing LTM (eds) An anthology of theories and models of design: philosophy, approaches and empirical explorations. Springer, London, London, pp 327–352

Zimmermann M, von Hoessle JE (2013) Computing solution spaces for robust design. Numer Methods Eng 94:290–307. https://doi.org/10.1002/nme.4450